Sensors and Actuators B 171–172 (2012) 1110–1116

Contents lists available at SciVerse ScienceDirect

Sensors and Actuators B: Chemical

journal homepage: www.elsevier.com/locate/snb

New water-soluble highly selective fluorescent chemosensor for Fe (III) ions and its application to living cell imaging

Shi-Rong Liu, Shu-Pao Wu*

Department of Applied Chemistry, National Chiao Tung University, Hsinchu 300, Taiwan, ROC

ARTICLE INFO

Article history:
Received 19 April 2012
Received in revised form 14 June 2012
Accepted 18 June 2012
Available online 27 June 2012

Keywords:
Sensors
Iron
Rhodamine
Imaging agents

ABSTRACT

A new rhodamine-based chemosensor exhibits excellent selectivity for Fe^{3+} ions over a wide range of tested metal ions Ag^{+}, Al^{3+}, Ca^{2+}, Cd^{2+}, Co^{2+}, Cr^{3+}, Cu^{2+}, Fe^{2+}, Hg^{2+}, Mg^{2+}, Mn^{2+}, Ni^{2+}, Pb^{2+}, and Zn^{2+} in an aqueous solution. The binding of Fe^{3+} to chemosensor **1** produces an absorption band at 564 nm and an emission band at 588 nm because Fe^{3+}-binding induces ring-opening of the spirolactam in **1**. The binding ratio of the **1**–Fe^{3+} complexes was determined to be 1:1 according to a Job plot. The association constant (K_a) of Fe^{3+} binding in chemosensor **1** was 6.9×10^3 M^{-1}. The maximum fluorescence enhancement caused by Fe^{3+} binding in chemosensor **1** occurred at a pH range of 6–7.5. The fluorescence microscopy experiments in this study demonstrated that chemosensor **1** can be used as a fluorescent probe for detecting Fe^{3+} in living cells.

1. Introduction

The development of chemosensors for detecting biologically and environmentally important metal ions, such as Cu^{2+}, Fe^{3+}, Zn^{2+}, Cd^{2+}, Hg^{2+}, and Pb^{2+}, has been an important research topic [1–8]. Iron is the most abundant essential transition metal ion in humans, and acts as a cofactor for many proteins in a wide range of biochemical processes. These processes include oxygen transport, electron transport, and oxidoreductase catalysis [9]. The regulation of iron in the human body is a highly controlled process. Iron deficiency leads to low oxygen delivery to cells, resulting in anemia, low blood pressure, and decreased immunity [10]. Conversely, an overload of iron ions in a living cell can trigger the formation of reactive oxygen species (ROS) through the Fenton reaction. These ROS can damage lipids, nucleic acids, and proteins. The cellular toxicity caused by iron ions has been linked with several serious diseases, such as Alzheimer's, Huntington's, and Parkinson's diseases [11–13].

Researchers have developed several traditional methods of measuring iron ions in various samples, including atomic absorption spectrometry [14], inductively coupled plasma mass spectroscopy (ICPMS) [15], inductively coupled plasma-atomic emission spectrometry (ICP-AES) [16], and voltammetry [17]. Although these methods are quantitative, they require the sophisticated apparatus, and are not easily employed in on-site analysis. Researchers have recently focused on the development of selective and sensitive sensors for iron detection [18–31].

Because of the paramagnetic nature of Fe^{3+}, most reported fluorescent Fe^{3+} chemosensors are based on a fluorescence quenching mechanism [32–36]. The design of "off-on" fluorescent Fe^{3+} chemosensors remains a challenging task. Rhodamine-based chemosensors provide a solution to the fluorescence-quenching effect caused by metal ion binding. Rhodamine derivatives undergo equilibrium between spirolactam (nonfluorescence) and ring-opened amide (fluorescence) forms, providing an ideal model for the design of metal ion sensing with light "off-on" switching. Metal ion binding triggers ring-opening of rhodamine and produces a red emission. Unfortunately, most of the currently existing rhodamine-based sensors for Fe(III) ions are undesirably insoluble in an aqueous solution. In order to resolve this solubility issue – a major obstacle in the fabrication of water soluble metal ion chemosensors – the development of suitable water-soluble metal-binding receptors is very useful as these can be used for highly sensitive analysis in living cells.

This study designed a rhodamine-based fluorescent chemosensor for metal ion detection in an aqueous solution. Chemosensor **1** was synthesized by the condensation of rhodamine-B hydrazine and 2-(*N*-methylpiperazinylimino)acetaldehyde (Scheme 1). Chemosensor **1** is colorless and exhibits weak fluorescence. Binding metal ions to chemosensor **1** induced ring-opening of rhodamine. This resulted in a red emission and a color change from colorless to pink because of a shift in the equilibrium state from a spirolactam to a ring-open amide. The metal ions Ag^{+}, Al^{3+}, Ca^{2+}, Cd^{2+}, Co^{2+}, Cr^{3+}, Cu^{2+}, Fe^{2+}, Fe^{3+}, Hg^{2+}, Mg^{2+}, Mn^{2+}, Ni^{2+}, Pb^{2+}, and Zn^{2+} were tested for metal ion binding selectivity with chemosensor **1**, but Fe^{3+} was the only ion that caused a visible color change (from colorless to pink) and a red emission after binding

* Corresponding author.
E-mail address: spwu@mail.nctu.edu.tw (S.-P. Wu).

0925-4005/$ – see front matter © 2012 Elsevier B.V. All rights reserved.
http://dx.doi.org/10.1016/j.snb.2012.06.041

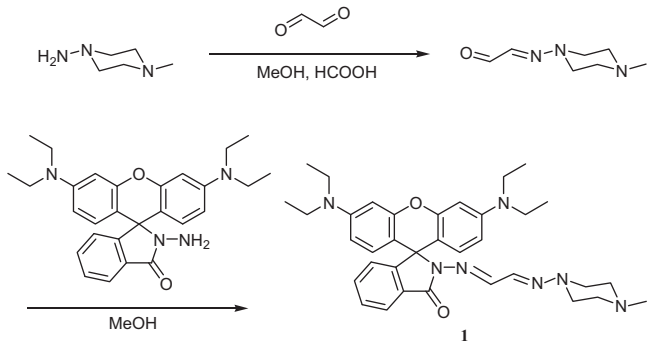

Scheme 1. Synthesis of chemosensor **1**.

with chemosensor **1**. The fluorescence microscopy experiments in this study also demonstrated that chemosensor **1** can be used as a fluorescent probe for detecting Fe^{3+} in living cells.

2. Materials and methods

2.1. Materials and instrumentation

All reagents were obtained from commercial sources and used as received without further purification. UV/Vis spectra were recorded on an Agilent 8453 UV/Vis spectrometer. Fluorescence spectra measurements were performed on a Hitachi F-7000 fluorescence spectrophotometer. NMR spectra were obtained on a Bruker DRX-300 and DRX-500 NMR spectrometer. Fluorescent pictures were taken on a ZEISS Axio Scope A1 Fluorescence Microscope.

2.2. Synthesis of 2-(N-methylpiperazinylimino)acetaldehyde

Glyoxal (232.8 mg, 4.0 mmol, dissolved in 20 mL MeOH) and formic acid (0.5 mL) were slowly added to a solution of 1-amino-4-methylpiperazine (115.0 mg, 1.0 mmol) in 10 mL MeOH. The reaction mixture was stirred at room temperature for 6 h. The solvent was evaporated under reduced pressure, and the crude product was purified by column chromatography (ethyl acetate: methanol = 1:1) to give the compound as a yellow oil. Yield: 116 mg (75%). ^{1}H NMR (300 MHz, CD_3OD): δ 9.35 (d, J = 7.2 Hz, 1H), 7.02 (d, J = 7.5 Hz, 1H), 3.52 (t, J = 5.4 Hz, 4H), 2.67 (t, J = 5.4 Hz, 4H), 2.40 (s, 3H). ^{13}C NMR (75 MHz, CD_3OD): δ 191.9, 131.2, 53.8, 49.8, 44.9. MS (EI): m/z (%) = 155.1 (19), 99.1 (100) 56.0 (97). HRMS (EI): m/z calcd for $C_7H_{13}N_3O$ 155.1059; found 155.1054.

2.3. Synthesis of chemosensor **1**

2-(*N*-methylpiperazinylimino)acetaldehyde (155 mg, 1.0 mmol) was added to the solution of rhodamine B hydrazine (547 mg, 1.2 mmol) in 15 mL MeOH. The reaction mixture was stirred at room temperature for 4 h. The solvent was evaporated under reduced pressure, and the crude product was purified by column chromatography (ethyl acetate:methanol = 2:1) to give compound **1** as a dark red solid. Yield: 273 mg (46%); m.p. 144–145 °C. ^{1}H NMR (500 MHz, CD_3OD): δ 7.88 (m, 2H), 7.49–7.43 (m, 2H), 7.07 (d, J = 7.5 Hz 1H), 6.93 (d, J = 7.5 Hz, 1H), 6.41 (d, J = 2.5 Hz, 2H), 6.37 (d, J = 9.0 Hz, 2H), 6.29 (dd, J = 2.5, 9.0 Hz, 2H), 3.31 (q, J = 7.0 Hz, 8H), 3.07 (t, J = 5.5 Hz, 4H), 2.50 (t, J = 5.5 Hz, 4H), 2.25 (s, 3H), 1.09 (t, J = 7.0 Hz, 12H). ^{13}C NMR (125 MHz, CD_3OD): δ 167.3, 154.4, 154.0, 150.5, 148.8, 135.2, 135.0, 129.7, 128.6, 128.4, 124.7, 124.1, 109.5, 105.9, 99.4, 67.4, 54.9, 50.7, 45.8, 45.3, 12.9. MS (FAB): m/z = 594.5 $[M+H]^+$. HRMS (FAB): calcd. for $C_{35}H_{43}N_7O_2$ 593.3478; found 593.3480.

2.4. The pH dependence on Fe^{3+} binding in chemosensor **1** studied by fluorescence spectroscopy

Chemosensor **1** (50 μM) was added with Fe^{3+} (200 μM) in 1.0 mL water–methanol solution (v/v = 9/1, 2 mM buffer). The buffers were: pH 3–4, KH_2PO_4–HCl; pH 5–6.5, Hepes; pH 7–10, Tris–HCl.

2.5. Determination of the binding stoichiometry and the association constants for the binding of Fe^{3+} to chemosensor **1**

The binding stoichiometry of the **1**–Fe^{3+} complex was determined from a Job plot [37]. The fluorescence intensity at 588 nm was plotted against the molar fraction of chemosensor **1** with a total concentration of the sensor and Fe^{3+} ion of 50 μM. The molar fraction at maximum emission intensity represents the binding stoichiometry of the **1**–Fe^{3+} complex. The maximum emission intensity was reached at a molar fraction of 0.5 (Fig. 5). This result indicates that chemosensor **1** forms a 1:1 complex with Fe^{3+}. The association constant (K_a) of **1**–Fe^{3+} complexes was determined by the Benesi–Hildebrand Eq. (1) [38,39]:

$$\frac{1}{F - F_0} = \frac{1}{\{K_a \times (F_{max} - F_0) \times [Fe^{3+}]\}} + \frac{1}{F_{max} - F_0}, \quad (1)$$

where F is the fluorescence intensity at 588 nm at any given Fe^{3+} concentration, F_0 is the fluorescence intensity at 588 nm in the absence of Fe^{3+}, and F_{max} is the maxima fluorescence intensity at 588 nm in the presence of Fe^{3+} in solution. The association constant K_a was evaluated graphically by plotting $1/(F - F_0)$ against $1/[Fe^{3+}]$. Data were linearly fitted according to Eq. (1) and the K_a value was obtained from the slope and intercept of the line.

2.6. Cell culture

The cell line HeLa was provided by the Food Industry Research and Development Institute (Taiwan). HeLa cells were cultured in Dulbecco's modified Eagle's medium (DMEM) supplemented with 10% fetal bovine serum (FBS) at 37 °C under an atmosphere of 5% CO_2. Cells were plated on 18 mm glass coverslips and allowed to adhere for 24 h.

2.7. Fluorescence imaging

Experiments to assess the Fe^{3+} uptake were performed in phosphate-buffered saline (PBS) with 20 μM $FeCl_3$. The cells cultured in DMEM were treated with 10 mM solutions of $FeCl_3$ (2 μL; final concentration: 20 μM) dissolved in sterilized PBS (pH = 7.4) and incubated at 37 °C for 30 min. The treated cells were washed with PBS (2 mL × 3 mL) to remove remaining metal ions. DMEM (2 mL) was added to the cell culture, which was then treated with a 10 mM solution of chemosensor **1** (2 μL; final concentration: 20 μM) dissolved in DMSO. The samples were incubated at 37 °C for 30 min. The culture medium was removed, and the treated cells were washed with PBS (2 mL × 3 mL) before observation. Fluorescence imaging was performed with a ZEISS Axio Scope A1 fluorescence microscope. Cells loaded with chemosensor **1** were excited at 545 nm by using a 50 W Hg lamp. An emission filter of 570 nm was used.

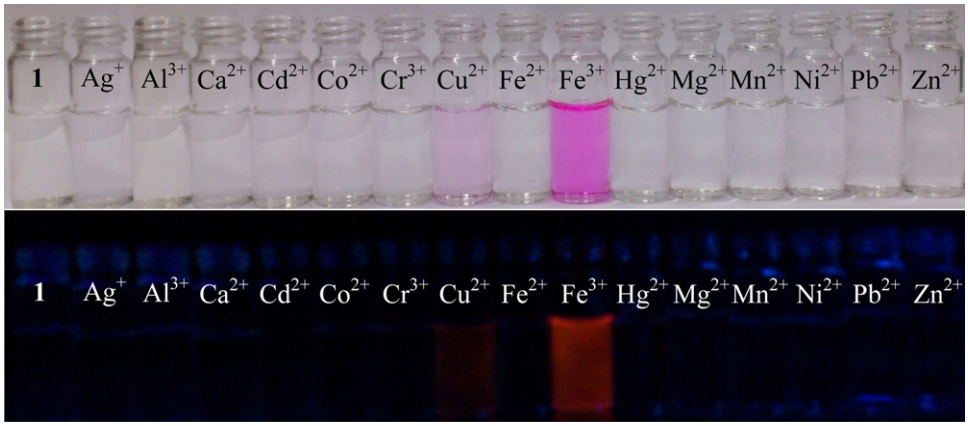

Fig. 1. Color (top) and fluorescence (For interpretation of the references to color in this figure legend, the reader is referred to the web version of the article.)(bottom) changes of Chemosensor **1** (50 μM) after addition of various metal ions (200 μM) in water–methanol (v/v = 9/1, 2 mM Tris–HCl, pH = 7.4) solution.

3. Results and discussion

3.1. Synthesis of chemosensor *1*

Scheme 1 outlines the procedure for synthesizing chemosensor **1**. 2-(*N*-methylpiperazinylimino)acetaldehyde was obtained from the reaction of 1-amino-4-methylpiperazine and glyoxal. Chemosensor **1** was synthesized through the reaction of rhodamine B hydrazide and 2-(*N*-methylpiperazinylimino) acetaldehyde, which formed an imine bond. The structure of chemosensor **1** was confirmed using ^{1}H NMR, ^{13}C NMR, and MS spectra (see supplementary data). Chemosensor **1** is colorless and nonfluorescent, indicating that the spirocyclic form of **1** was retained in solution.

3.2. Cation-sensing properties

The sensing ability of chemosensor **1** was tested by mixing it with the metal ions Ag^{+}, Al^{3+}, Ca^{2+}, Cd^{2+}, Co^{2+}, Cr^{3+}, Cu^{2+}, Fe^{2+}, Fe^{3+}, Hg^{2+}, Mg^{2+}, Mn^{2+}, Ni^{2+}, Pb^{2+}, and Zn^{2+}. The Fe^{3+} ion was the only ion to cause a change in color (from colorless to pink) and red fluorescence in chemosensor **1** (Fig. 1). Other metal ions produced minor changes or no changes in color and fluorescence. The quantitative fluorescence spectra of chemosensor **1** were recorded in the presence of several metal ions. Fe^{3+} was the only metal ion to cause a significant emission (Fig. 2). Cu^{2+} also caused an emission peak, but its intensity was relatively lower than that caused by Fe^{3+}.

Fe^{3+} titration against chemosensor **1** was monitored using UV–vis and fluorescence spectra (Fig. 3). The UV–vis spectra show a new absorption band at 564 nm during Fe^{3+} titration. Fe^{3+} binding with chemosensor **1** caused the ring-opening of rhodamine

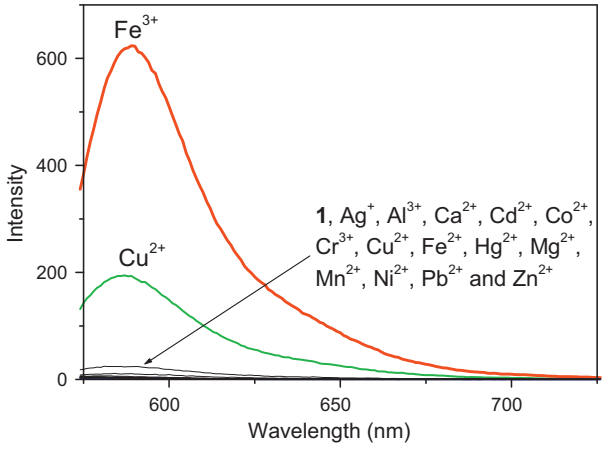

Fig. 2. Fluorescence response of **1** (50 μM) to different metal ions (200 μM) in a water–methanol (v/v = 9/1, 2 mM Tris–HCl, pH = 7.4) solution. The excitation wavelength was 564 nm.

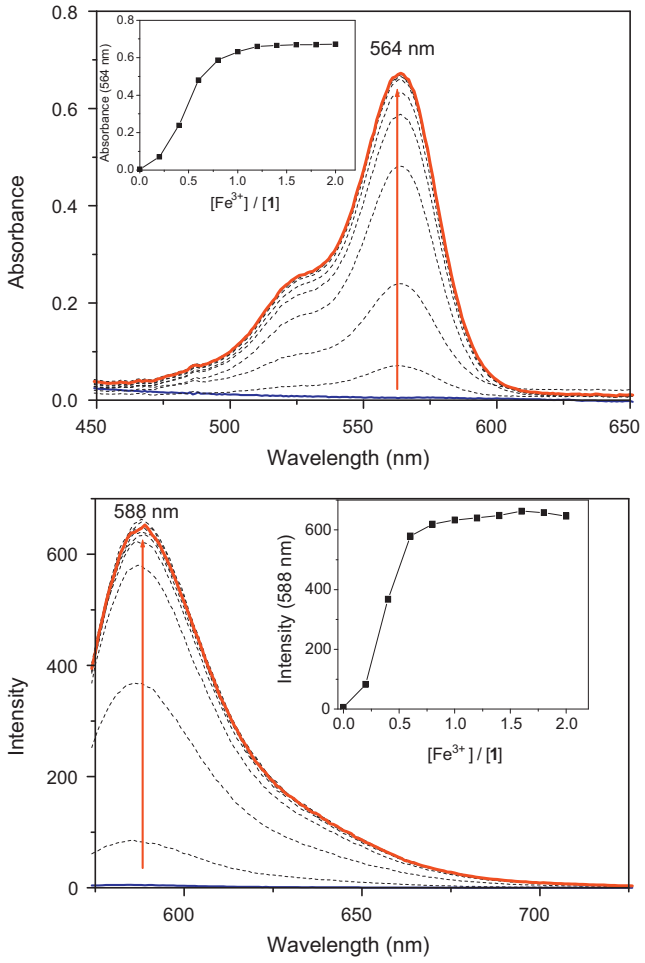

Fig. 3. Absorption (up) and fluorescence (bottom) changes of chemosensor **1** (50 μM) in the presence of various equivalents of Fe^{3+} in a water–methanol (v/v = 9/1) solution. The excitation wavelength was 564 nm. (For interpretation of the references to color in this figure legend, the reader is referred to the web version of the article.)

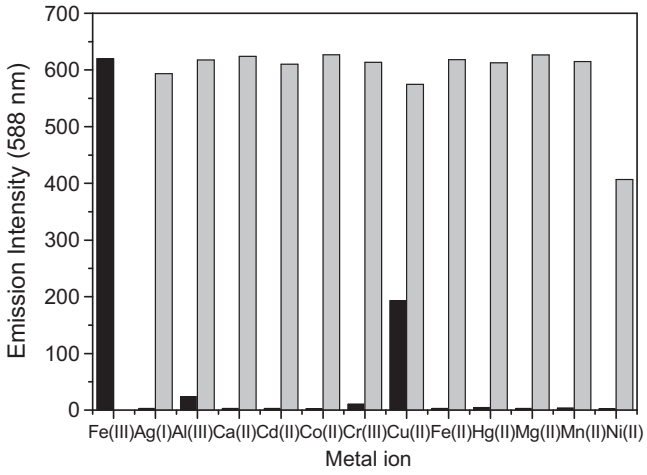

Fig. 4. Fluorescence response of Chemosensor **1** (50 μM) to Fe^{3+} (200 μM) or 200 μM of other metal ions (the black bar portion) and to the mixture of other metal ions (200 μM) with 200 μM of Fe^{3+} (the gray bar portion) in water–methanol (v/v = 9:1, 2 mM Tris–HCl, pH = 7.4) solutions.

and produced a color change from colorless to pink. Fluorescence spectra show that Fe^{3+} addition to chemosensor **1** caused a new emission band centered at 588 nm, which appeared as a red emission. The emission intensity reached its maximum after the addition of one equivalent of Fe^{3+}. The quantum yield of the emission band was $\Phi = 0.303$, which is 34-fold higher than that of chemosensor **1**, at $\Phi = 0.009$. These results indicate that Fe^{3+} is the only metal ion that readily binds to chemosensor **1**, causing significant fluorescence enhancement and permitting the highly selective detection of Fe^{3+}.

To further evaluate the selectivity of chemosensor **1** toward various metal ions, competitive experiments were conducted to study the influence of other metal ions on Fe^{3+} binding with chemosensor **1** (Fig. 4). The fluorescence enhancement caused by mixing Fe^{3+} (200 μM) with most metal ions (200 μM) was similar to that caused by Fe^{3+} alone. A smaller enhancement of the fluorescence intensity was observed only when Fe^{3+} was mixed with Ni^{2+}, indicating that Ni^{2+} competes with Fe^{3+} for binding with chemosensor **1**. These results indicate the high selectivity of chemosensor **1** for Fe^{3+} over other competitive metal ions in a water–methanol solution.

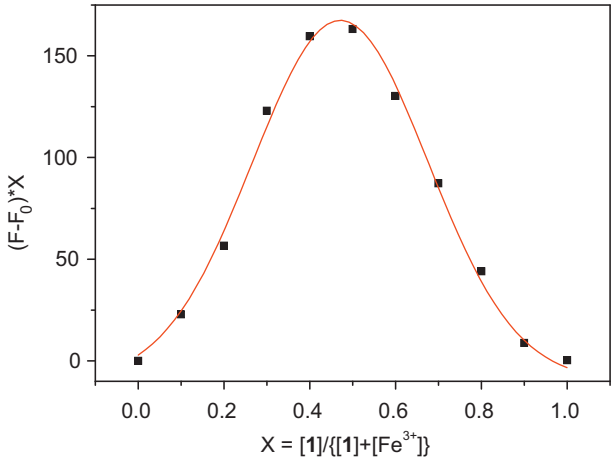

Fig. 5. Job plot of the **1**–Fe^{3+} complexes in a water–methanol (v/v = 9/1) solution. The monitored wavelength is 588 nm. The total concentration of Chemosensor **1** and Fe^{3+} was 50 μM.

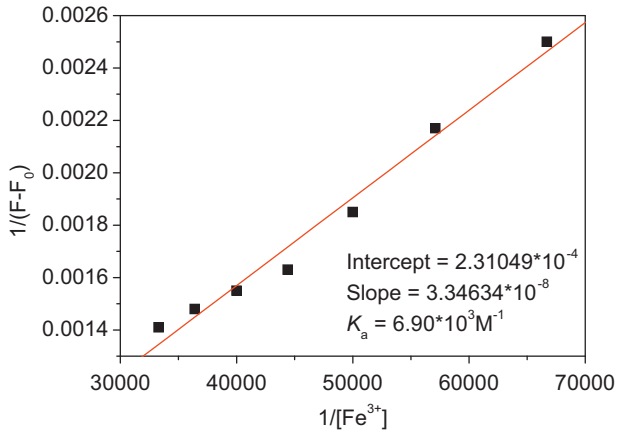

Fig. 6. Benesi–Hildebrand plot of **1**–Fe^{3+} complexes in a water–methanol (v/v = 9/1) solution.

To determine the binding stoichiometry of the **1**–Fe^{3+} complex, the emission intensity of chemosensor **1** at 588 nm was plotted as a function of its molar fraction under a constant total concentration. Fig. 5 shows the resulting Job plot. The maximum emission intensity was reached at a molar fraction of 0.5. This indicates a 1:1 ratio for the **1**–Fe^{3+} complex (i.e., one Fe^{3+} ion binds to one molecule of chemosensor **1**). The formation of a 1:1 **1**–Fe^{3+} complex was confirmed by ESI-MS, in which the peak at $m/z = 719.3$ indicates a 1:1 stoichiometry for the $[\mathbf{1} + FeCl_2]^+$ complex (see Fig. S5 in the supplementary data). The association constant K_a of the **1**–Fe^{3+} complex was evaluated graphically by plotting $1/\Delta F$ against $1/[Fe^{3+}]$ (Fig. 6). The data were linearly fitted to the Benesi–Hildebrand equation and the K_a value was obtained from the slope and intercept of the line. The association constant (K_a) for Fe^{3+} binding in chemosensor **1** was determined to be $6.90 \times 10^3\ M^{-1}$. The detection limit of chemosensor **1** as a fluorescent sensor for the analysis of Fe^{3+} was determined from the plot of fluorescence intensity as a function of the concentration of Fe^{3+} (see Fig. 7). It was found that chemosensor **1** has a detection limit of 2.2 μM, which is allowed for the detection of micromolar concentration range of Fe^{3+}.

To gain a clearer understanding of the structure of **1**–Fe^{3+} complexes, ^1H NMR spectroscopy (Fig. 8) was employed. Fe^{3+} is a

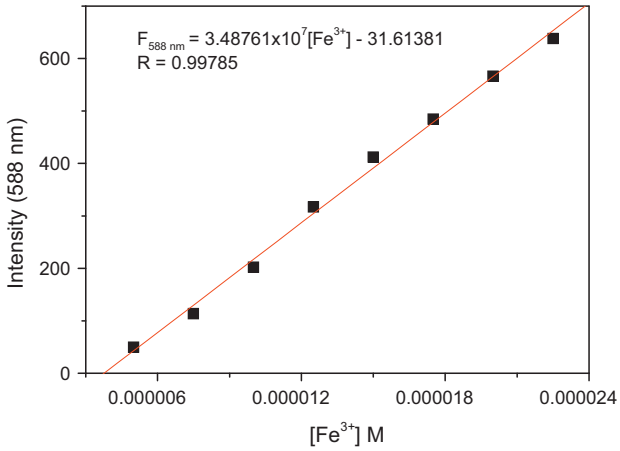

Fig. 7. Calibration curve of **1**–Fe^{3+} in a water–methanol (v/v = 9/1) solution. The excitation wavelength was 564 nm and the monitored emission wavelength was 588 nm. The detection limit (DL) of Fe^{3+} ions using chemosensor **1** was determined from the following equation: $DL = K \times SD/S$, where $K = 3$; SD is the standard deviation of the blank solution; S is the slope of the calibration curve. $DL = K \times SD/S = 3 \times 26.02306/3.48761 \times 10^7 = 2.2 \times 10^{-6}$ M.

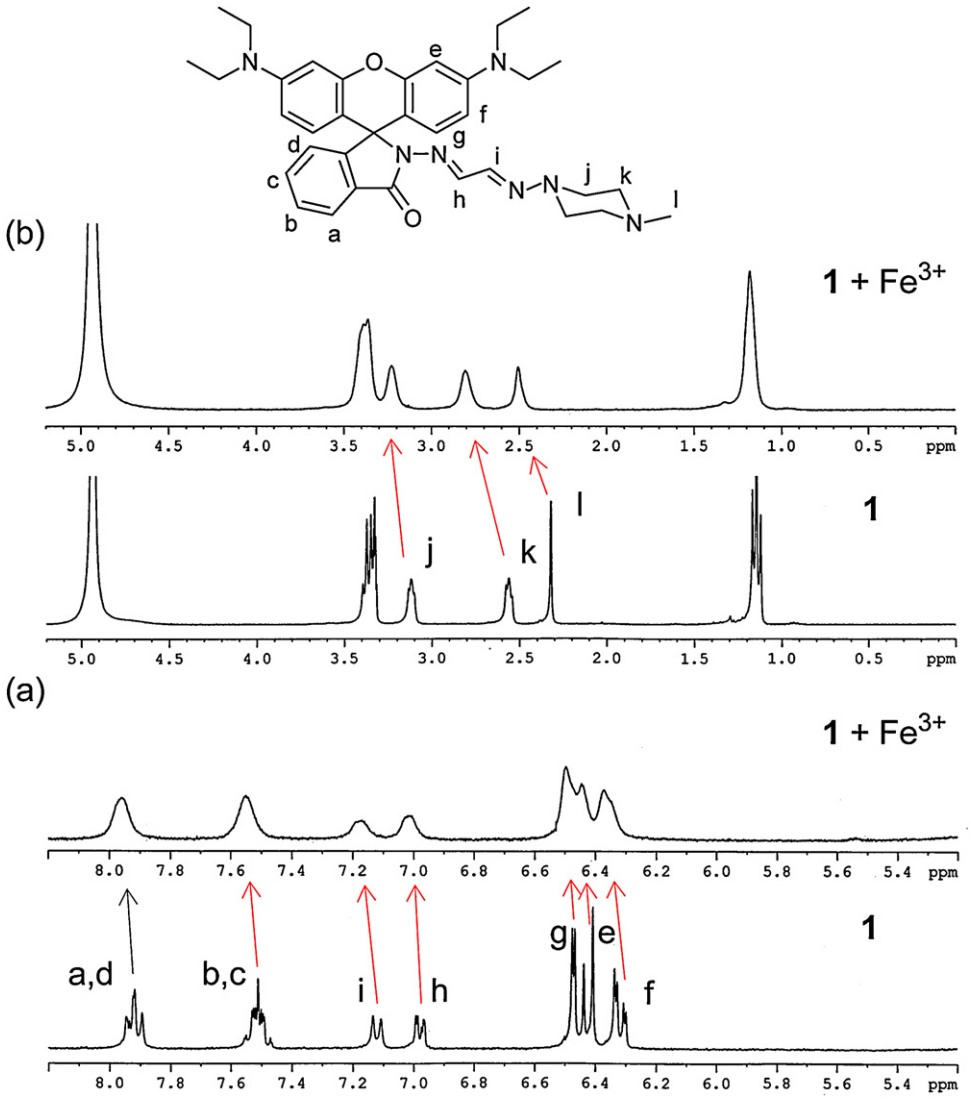

Fig. 8. ^{1}H NMR spectra of chemosensor **1** (10 mM) in the presence of 1 equivalent of Fe^{3+} in CD_3OD.

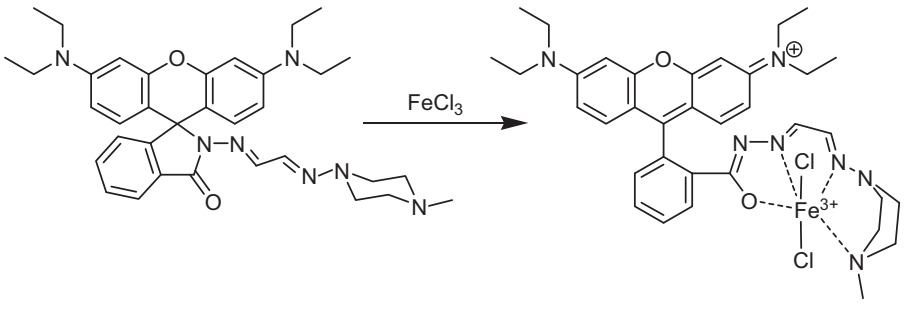

Fig. 9. A proposed 1:1 complex formed between **1** and Fe^{3+}.

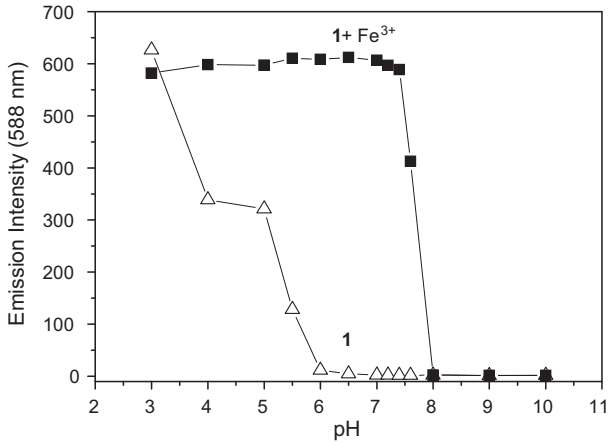

Fig. 10. Fluorescence response (588 nm) of free Chemosensor **1** (50 μM) (▲) and after addition of Fe^{3+} (200 μM) (■) in a water–methanol (v/v = 9:1, 2 mM buffer) solution as a function of different pH values. (For interpretation of the references to color in this figure legend, the reader is referred to the web version of the article.)

paramagnetic metal ion and can affect the proton signals that are close to the Fe^{3+} binding site. The proton signals H_e, H_f and H_g are shifted downfield upon addition of Fe^{3+}. This indicated the opening of the spirolactam ring upon coordination to Fe^{3+} with associated charge transfer in the xanthene moiety. The proton signals H_h, H_i, H_j, H_k and H_l are also shifted downfield upon addition of Fe^{3+}. These observations show that Fe^{3+} binds to chemosenor **1** through one oxygen atom, two imine nitrogen atoms, and one nitrogen atom at a piperazine moiety (Fig. 9).

A pH titration of chemosensor **1** was conducted to investigate a suitable pH range for Fe^{3+} sensing. Fig. 10 shows that the emission intensities of metal-free chemosensor **1** are low, at a pH range of 6–10. The emission intensity increases dramatically when the pH value is lower than 4. This is because of protonation-induced ring opening in chemosensor **1**. After mixing chemosensor **1** with Fe^{3+}, the emission intensity at 588 nm is markedly higher at a pH range of 3.0–7.5. The emission intensity decreases at pH > 7.5. This indicates poor stability of the **1**–Fe^{3+} complexes at high pH values. Because chemosensor **1** undergoes ring-opening at low pH, the best pH range for Fe^{3+} sensing is approximately 6–7.5.

3.3. Living cell imaging

Chemosensor **1** was used for living cell imaging. To detect Fe^{3+} in living cells, HeLa cells were cultured in DMEM supplemented with 10% FBS at 37 °C and 5% CO_2. Cells were plated on 18 mm glass coverslips and allowed to adhere for 24 h. HeLa cells were treated with 20 μM $FeCl_3$ for 30 min and washed with PBS 3 times. The cells were then incubated with chemosensor **1** (20 μM) for 30 min and washed with PBS to remove the remaining sensor. The images of the HeLa cells were obtained using a fluorescence microscope. Fig. 11 shows the images of HeLa cells with chemosensor **1** after treatment of Fe^{3+}. An overlay of fluorescence and bright-field images shows that the fluorescence signals are localized in the intracellular area, indicating a subcellular distribution of Fe^{3+} and good cell-membrane permeability of chemosensor **1**.

4. Conclusion

The new fluorescence chemosensor **1** displays an excellent selectivity for Fe^{3+} ions over competing metal ions. The fluorescence of chemosensor **1** was significantly enhanced in the presence of Fe^{3+}, and the addition of Ag^{+}, Al^{3+}, Ca^{2+}, Cd^{2+}, Co^{2+}, Cr^{3+}, Cu^{2+}, Fe^{2+}, Hg^{2+}, Mg^{2+}, Mn^{2+}, Ni^{2+}, Pb^{2+}, or Zn^{2+} barely affected the fluorescence. This rhodamine-based Fe^{3+} chemosensor is also an effective method for Fe^{3+} sensing in living cell imaging.

Acknowledgments

We gratefully acknowledge the financial support of the National Science Council (ROC) and National Chiao Tung University.

Appendix A. Supplementary data

Supplementary data associated with this article can be found, in the online version, at http://dx.doi.org/10.1016/j.snb.2012.06.041.

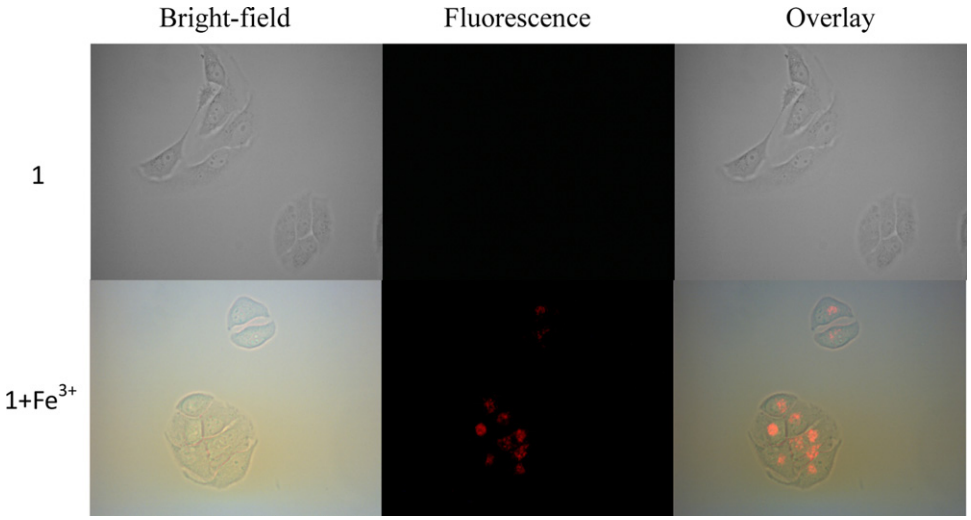

Fig. 11. Fluorescence images of HeLa cells treated with **1** and $FeCl_3$. (left) Bright field image; (middle) fluorescence image; and (right) merged image. (For interpretation of the references to color in this figure legend, the reader is referred to the web version of the article.)

References

[1] A.P. de Silva, H.Q.N. Gunaratne, T. Gunnlaugsson, A.J.M. Huxley, C.P. McCoy, J.T. Rademacher, T.E. Rice, Signaling recognition events with fluorescent sensors and switches, Chemical Reviews 97 (1997) 1515–1566.

[2] E.M. Nolan, S.J. Lippard, Tools and tactics for the optical detection of mercuric ion, Chemical Reviews 108 (2008) 3443–3480.

[3] H.S. Hewage, E.V. Anslyn, Pattern-based recognition of thiols and metals using a single squaraine indicator, Journal of the American Chemical Society 131 (2009) 13099–13106.

[4] N. Kaur, S. Kumar, Colormetric metal ion sensors, Tetrahedron 67 (2011) 9233–9264.

[5] G. Kuang, J.R. Allen, M.A. Baird, B.T. Nguyen, L. Zhang, T.J. Morgan Jr., C.W. Levenson, M.W. Davidson, L. Zhu, Balance between fluorescence enhancement and association affinity in fluorescent heteroditopic indicators for imaging zinc ion in living cells, Inorganic Chemistry 50 (2011) 10493–10504.

[6] M. Dutta, D. Das, Recent developments in fluorescent sensors for trace-level determination of toxic-metal ions, Trends in Analytical Chemistry 32 (2012) 113–132.

[7] H.N. Kim, W.X. Ren, J.S. Kim, J. Yoon, Fluorescent and colorimetric sensors for detection of lead, cadmium, and mercury ions, Chemical Society Reviews 41 (2012) 3210–3244.

[8] A. Barba-Bon, A.M. Costero, S. Gil, M. Parra, J. Soto, R. Martinez-Manez, F. Sancenon, A new selective fluorogenic probe for trivalent cations, Chemical Communications 48 (2012) 3000–3002.

[9] J.A. Cowan, Inorganic Biochemistry: an Introduction, Wiley-VCH, New York, 1997, pp. 167–255.

[10] J.D. Haas, T. Brownlie IV, Iron deficiency and reduced work capacity: a critical review of the research to determine a causal relationship, Journal of Nutrition 131 (2001) 676s–688s.

[11] J.R. Burdo, J.R. Connor, Brain iron uptake and homeostatic mechanisms: an overview, BioMetals 16 (2003) 63–75.

[12] D.J. Bonda, H. Lee, J.A. Blair, X. Zhu, G. Perryab, M.A. Smith, Role of metal dyshomeostasis in Alzheimer's disease, Metallomics 3 (2011) 267–270.

[13] A.S. Pithadia, M.H. Lee, Metal-associated amyloid-β species in Alzheimer's disease, Current Opinion in Chemical Biology 16 (2012) 67–73.

[14] J.E.T. Andersen, A novel method for the filterless preconcentration of iron, Analyst 130 (2005) 385–390.

[15] M.E. del Castillo Busto, M. Montes-Bayon, E. Blanco-Gonzalez, J. Meija, A. Sanz-Medel, Strategies to study human serum transferrin isoforms using integrated liquid chromatography ICPMS, MALDI-TOF, and ESI-Q-TOF detection: application to chronic alcohol abuse, Analytical Chemistry 77 (2005) 5615–5621.

[16] K. Pomazal, C. Prohaska, I. Steffan, G. Reich, J.F.K. Huber, Determination of Cu, Fe, Mn, and Zn in blood fractions by SEC–HPLC–ICP–AES coupling, Analyst 124 (1999) 657–663.

[17] C.M.G van den Berg, Chemical speciation of iron in seawater by cathodic stripping voltammetry with dihydroxynaphthalene, Analytical Chemistry 78 (2006) 156–163.

[18] J.L. Bricks, A. Kovalchuk, C. Trieflinger, M. Nofz, M. Büschel, A.I. Tolmachev, J. Daub, K. Rurack, On the development of sensor molecules that display Fe^{III}-amplified fluorescence, Journal of the American Chemical Society 127 (2005) 13522–13529.

[19] Y. Xiang, A. Tong, A new rhodamine-based chemosensor exhibiting selective Fe^{III}-amplified fluorescence, Organic Letters 8 (2006) 1549–1552.

[20] M. Zhang, Y. Gao, M. Li, M. Yu, F. Li, L. Li, M. Zhu, J. Zhang, T. Yi, C. Huang, A selective turn-on fluorescent sensor for Fe^{III} and application to bioimaging, Tetrahedron Letters 48 (2007) 3709–3712.

[21] B. Wang, J. Hai, Z. Liu, Q. Wang, Z. Yang, S. Sun, Selective detection of iron(III) by rhodamine-modified Fe_3O_4 nanoparticles, Angewandte Chemie International Edition 49 (2010) 4576–4579.

[22] D.P. Kennedy, C.D. Incarvito, S.C. Burdette, FerriCast: a macrocyclic photocage for Fe^{3+}, Inorganic Chemistry 49 (2010) 916–923.

[23] L. Zhang, J. Zhao, X. Zeng, L. Mu, X. Jiang, M. Deng, J. Zhang, G. Wei, Tuning with pH: the selectivity of a new rhodamine B derivative chemosensor for Fe^{3+} and Cu^{2+}, Sensors and Actuators B 160 (2011) 662–669.

[24] A.J. Weerasinghe, F.A. Abebe, E. Sinn, Rhodamine based turn-ON dual sensor for Fe^{3+} and Cu^{2+}, Tetrahedron Letters 52 (2011) 5648–5651.

[25] S. Wang, X. Meng, M. Zhu, A naked-eye rhodamine-based fluorescent probe for Fe(III) and its application in living cells, Tetrahedron Letters 52 (2011) 2840–2843.

[26] L. Zhang, J. Wang, J. Fan, K. Guo, X. Peng, A highly selective, fluorescent chemosensor for bioimaging of Fe^{3+}, Bioorganic & Medicinal Chemistry Letters 21 (2011) 5413–5416.

[27] D. Wei, Y. Sun, J. Yin, G. Wei, Y. Du, Design and application of Fe^{3+} probe for "naked-eye" colorimetric detection in fully aqueous system, Sensors and Actuators B 160 (2011) 1316–1321.

[28] E. Hao, T. Meng, M. Zhang, W. Pang, Y. Zhou, L. Jiao, Solvent dependent fluorescent properties of a 1, 2,3-triazole linked 8-hydroxyquinoline chemosensor: tunable detection from Zinc(II) to Iron(III) in the CH_3CN/H_2O system, Journal of Physical Chemistry A 115 (2011) 8234–8241.

[29] Z. Yang, M. She, B. Yin, J. Cui, Y. Zhang, W. Sun, J. Li, Z. Shi, Three rhodamine-based "off-on" chemosensors with high selectivity and sensitivity for Fe^{3+} imaging in living cells, Journal of Organic Chemistry 77 (2012) 1143–1147.

[30] M. Kumar, R. Kumar, V. Bhalla, P.R. Sharma, T. Kaur, Y. Qurishi, Thiacalix[4]arene based fluorescent probe for sensing and imaging of Fe^{3+} ions, Dalton Transactions 41 (2012) 408–412.

[31] Z. Li, L. Zhang, X. Li, Y. Guo, Z. Ni, J. Chen, L. Wei, M. Yu, A fluorescent color/intensity changed chemosensor for Fe^{3+} by photo-induced electron transfer (PET) inhibition of fluoranthene derivative, Dyes and Pigments 94 (2012) 60–65.

[32] F. Thomas, G. Serratrice, C. Beguin, E.S. Aman, J.L. Pierre, M. Fontecave, J.P. Laulhere, Calcein as a fluorescent probe for ferric iron, Journal of Biological Chemistry 274 (1999) 13375–13383.

[33] J.M. Liu, J.L. Yang, C.F. Chen, Z.T. Huang, A new fluorescent chemosensor for Fe^{3+} and Cu^{2+} based on calix[4]arene, Tetrahedron Letters 43 (2002) 9209–9212.

[34] Y. Ma, W. Luo, P.J. Quinn, Z. Liu, R.C. Hider, Design, synthesis, physicochemical properties, and evaluation of novel iron chelators with fluorescent sensors, Journal of Medicinal Chemistry 47 (2004) 6349–6362.

[35] G.E. Tumambac, C.M. Rosencrance, C. Wolf, Selective metal ion recognition using a fluorescent 1, 8-diquinolylnaphthalene-derived sensor in aqueous solution, Tetrahedron 60 (2004) 11293–11297.

[36] J.P. Sumner, R. Kopelman, Alexa Fluor 488 as an iron sensing molecule and its application in PEBBLE nanosensors, Analyst 130 (2005) 528–533.

[37] A. Senthilvelan, I. Ho, K. Chang, G. Lee, Y. Liu, W. Chung, Cooperative recognition of a copper cation and anion by a calix[4]arene substituted at the lower rim by a β-amino-α,β-unsaturated ketone, Chemistry: A European Journal 15 (2009) 6152–6160.

[38] H.A. Benesi, J.H. Hildebrand, A spectrophotometric investigation of the interaction of iodine with aromatic hydrocarbons, Journal of the American Chemical Society 71 (1949) 2703–2707.

[39] S. Wu, T. Wang, S. Liu, A highly selective turn-on fluorescent chemosensor for copper(II) ion, Tetrahedron 66 (2010) 9655–9658.

Biographies

Shi-Rong Liu is studying for Ph.D. in the department of Applied Chemistry at National Chiao Tung University. He received his MS in chemistry at National Chiao Tung University in 2009.

Shu-Pao Wu (Dr.) Corresponding Author Ph.D., 2004, Department of Chemistry, The Ohio State University, USA; Adviser: J.A. Cowan, Postdoctoral Fellow, 2004–2006, College of Chemistry, University of California, Berkeley, USA; Adviser: J.P. Klinman, Assistant Professor, 2006, National Chiao Tung University, Taiwan, Republic of China. Current interests: Metal ion chemosensors, AlkB.